

Role of Imaging Modalities and *N*-Acetylcysteine Treatment in Sepsis-Associated Encephalopathy

Yazhi Zhong,[#] Jitian Guan,[#] Yunfeng Ma, Meiling Xu, Yan Cheng, Liang Xu, Yan Lin, Xiaolei Zhang, and Renhua Wu*



Cite This: *ACS Chem. Neurosci.* 2023, 14, 2172–2182



Read Online

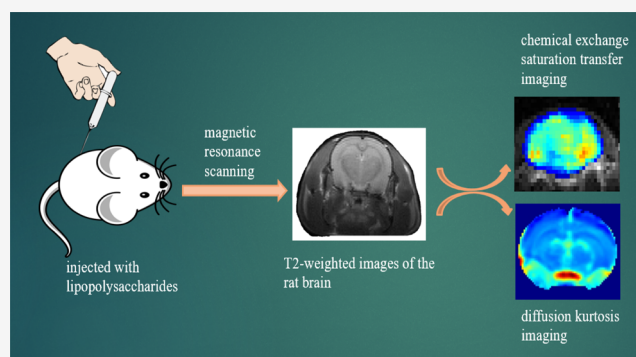
ACCESS |

Metrics & More

Article Recommendations

ABSTRACT: Sepsis-associated encephalopathy is a severe systemic infection complication. Although early stages involve pathophysiological changes, detection using conventional imaging is challenging. Glutamate chemical exchange saturation transfer and diffusion kurtosis imaging can noninvasively investigate cellular and molecular events in early disease stages using magnetic resonance imaging (MRI). *N*-Acetylcysteine, an antioxidant and precursor of glutathione, regulates neurotransmitter glutamate metabolism and participates in neuroinflammation. We investigated the protective role of *n*-acetylcysteine in sepsis-associated encephalopathy using a rat model and monitored changes in brain using magnetic resonance (MR) molecular imaging. Bacterial lipopolysaccharide was injected intraperitoneally to induce a sepsis-associated encephalopathy model. Behavioral performance was assessed using the open-field test. Tumor necrosis factor α and glutathione levels were detected biochemically. Imaging was performed using a 7.0-T MRI scanner. Protein expression, cellular damage, and changes in blood–brain barrier permeability were assessed using western blotting, pathological staining, and Evans blue staining, respectively. Lipopolysaccharide-induced rats showed reduced anxiety and depression after treatment with *n*-acetylcysteine. MR molecular imaging can identify pathological processes at different disease stages. Furthermore, rats treated with *n*-acetylcysteine showed increased glutathione levels and decreased tumor necrosis factor α , suggesting enhanced antioxidant capacity and inhibition of inflammatory processes, respectively. Western blot analysis showed reduced expression of nuclear factor kappa B (p50) protein after treatment, suggesting that *n*-acetylcysteine inhibits inflammation via this signaling pathway. Finally, *n*-acetylcysteine-treated rats showed reduced cellular damage by pathology and reduced extravasation of their blood–brain barrier by Evans Blue staining. Thus, *n*-acetylcysteine might be a therapeutic option for sepsis-associated encephalopathy and other neuroinflammatory diseases. Furthermore, noninvasive “dynamic visual monitoring” of physiological and pathological changes related to sepsis-associated encephalopathy was achieved using MR molecular imaging for the first time, providing a more sensitive imaging basis for early diagnosis, identification, and prognosis.

KEYWORDS: sepsis-associated encephalopathy, *N*-acetylcysteine, glutamate chemical exchange saturation transfer, diffusion kurtosis imaging, nuclear factor kappa B, neuroinflammation



INTRODUCTION

Sepsis is a severe systemic inflammatory reaction caused by bacterial toxins and can lead to organ dysfunction and exhaustion. Sepsis-associated encephalopathy is a commonly observed severe central nervous system (CNS) complication associated with systemic infection in patients with sepsis who show no evidence of a direct brain infection; however, inflammatory factors may enter the brain through the impaired blood–brain barrier and damage the nervous system.¹ Since sepsis-associated encephalopathy is associated with a high mortality rate (nearly 70%), early diagnosis and treatment are crucial.^{2–4} The etiology is multifactorial and involves pathological mechanisms, such as neuroinflammation (involvement of the immune cells [microglia and astrocytes]), damage to the neurons and myelin sheath, and neurotransmitter disorders (glutamate [Glu] and γ -aminobutyric acid). Furthermore, sepsis-associated encephalopathy may involve damage to the blood–brain barrier and microvessels.

ment of the immune cells [microglia and astrocytes]), damage to the neurons and myelin sheath, and neurotransmitter disorders (glutamate [Glu] and γ -aminobutyric acid). Furthermore, sepsis-associated encephalopathy may involve damage to the blood–brain barrier and microvessels.

Received: March 19, 2023

Accepted: May 4, 2023

Published: May 22, 2023



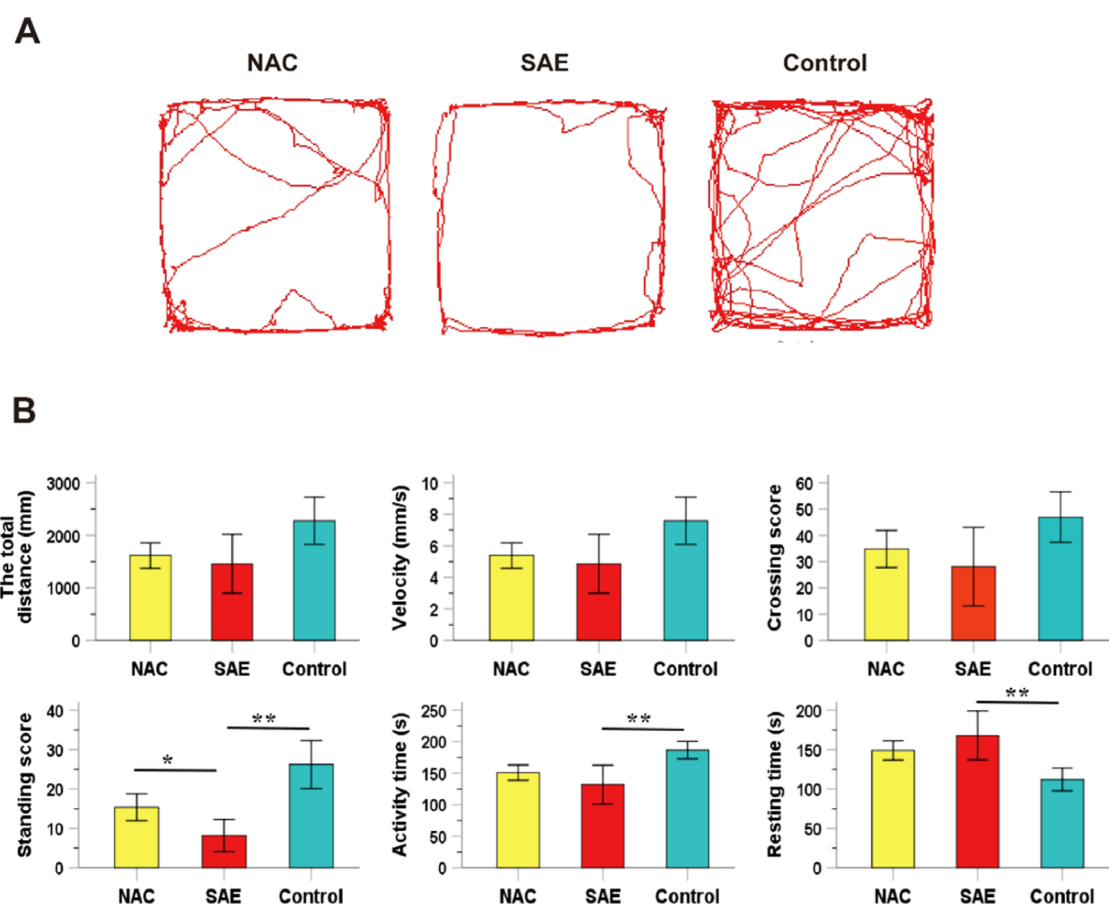


Figure 1. Results of the open-field test. (A) Images representing the motion trajectories in the open-field test for the three study groups. (B) Open-field test results of the three study groups.

The early clinical manifestations of sepsis-associated encephalopathy include disturbed mental status with no obvious abnormalities on conventional imaging. Microabscess and microthrombosis are late-stage complications associated with a significant increase in intensive care unit admission and mortality rates. Hence, alternative imaging techniques that can help in early diagnosis are of great clinical significance. In this context, magnetic resonance imaging (MRI)-based diffusion kurtosis imaging (DKI) and chemical exchange saturation transfer (CEST) imaging are advantageous as they can reveal intricate details of cellular and molecular damages.

DKI, an extension of the diffusion tensor imaging (DTI) technology, is a new magnetic resonance method based on the calculation of a non-gaussian model that can better depict the diffusion of the non-normal distribution of water molecules in tissues and better reflect the changes in the microscopic structures of the brain.⁵ The main parameters of DTI (fractional anisotropy [FA], mean diffusivity [MD], axial diffusion [Da], and radial diffusion [Dr]) can effectively show the demyelination changes in the brain under physiological or pathological conditions. The main parameters of DKI are mean kurtosis (MK), axial kurtosis (Ka), and radial kurtosis (Kr). Ka is more suitable for studying heterogeneous brain regions, such as the corpus callosum; the pathophysiological basis of Ka is related to the nerve fiber axons and endoplasmic reticulum disintegration. However, the background uniformity of Kr is worse than that of MK and Ka, affecting the utility of Kr during lesion detection and localization. MK has a relatively moderate background uniformity and contrast between tissues, effec-

tively detecting lesions and accurately locating and diagnosing lesions. Hence, MK is a more suitable DKI parameter for imaging isogenic brain regions, such as the cerebral cortex.⁶

CEST is another MRI technique that can detect endogenous and exogenous compounds containing exchangeable protons or biomolecules.⁷ A selective radiofrequency pulse saturates the exchangeable protons and transfers the saturation effect to the water molecules through a chemical exchange in CEST, causing a reduction in the MR signals of the water molecules and indirectly reflecting the substance concentration. Glu CEST acquires CEST signals of 3.0 ppm with a high irradiation power and is suggested to indicate Glu in the brain.⁸ Glu CEST may be associated with astrocyte proliferation in neuroinflammatory diseases, demonstrating its potential to be used as a neuroimaging biomarker for gliosis.⁹ Hence, DKI and Glu CEST may be used in combination to better reveal the physiological and pathological metabolic changes in the brain in sepsis-associated encephalopathy.

N-Acetylcysteine (NAC) is one of the precursors of glutathione and shows antioxidant and anti-inflammatory activities.¹⁰ NAC easily enters the CNS through the astrocytes, improves the intracellular antioxidant levels, and increases glutathione levels, thereby reducing oxidative stress.¹¹ NAC may inhibit the expression of tumor necrosis factor α (TNF- α) and interleukin-6 (IL-6) through the nuclear factor kappa B (NF κ B) signaling pathway, thereby preventing inflammation progression, delaying the course of the inflammatory disease in sepsis-associated encephalopathy, and improving clinical symptoms. Moreover, NAC also displays vasodilatory proper-

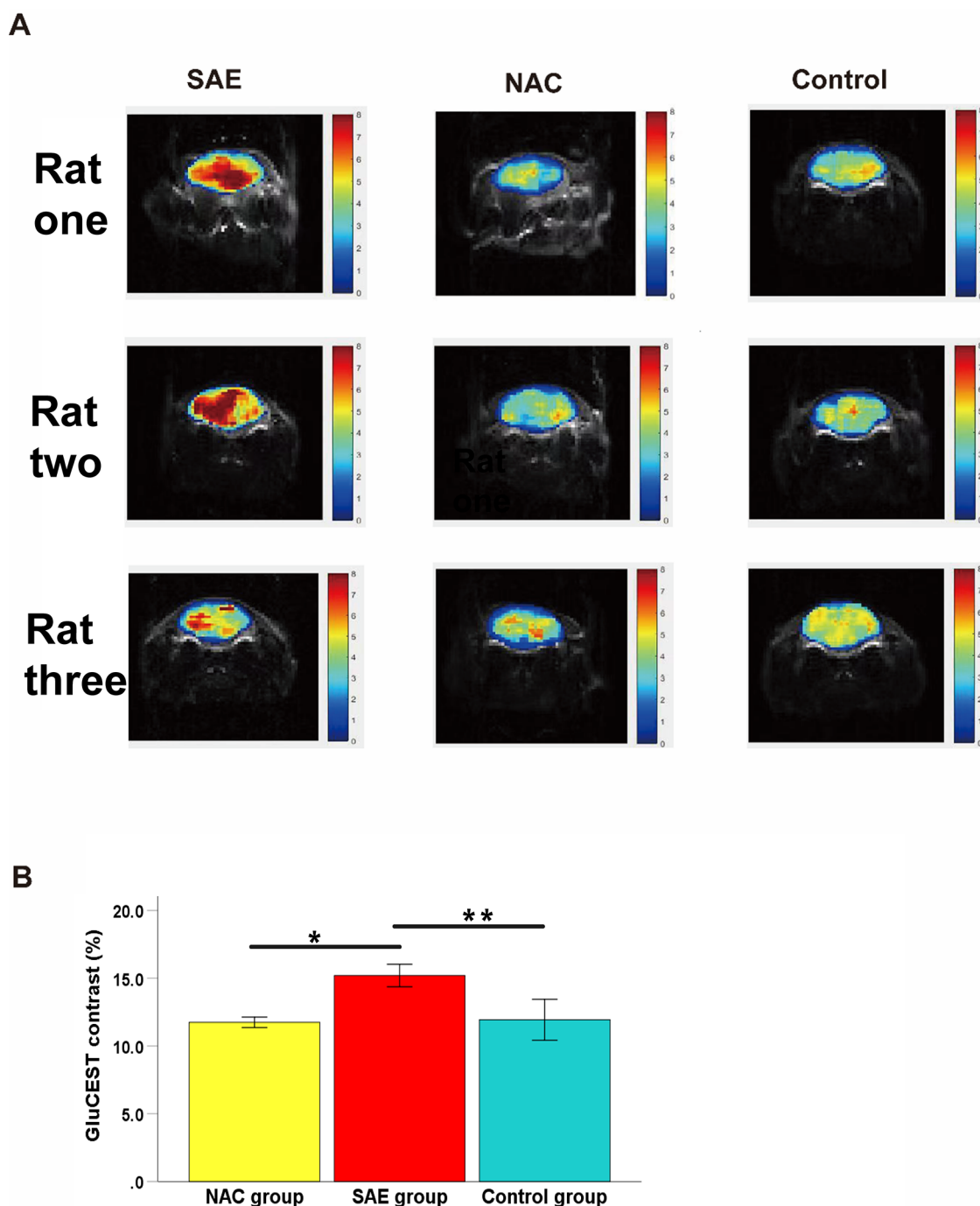


Figure 2. Results of Glu CEST. (A) Color map of Glu CEST for the three study groups. (B) Glu CEST estimation for the three study groups (* $P < 0.05$, ** $P < 0.01$). Glu CEST: Glutamate chemical exchange saturation transfer.

ties that benefit microcirculation in patients with sepsis.¹² A combination of NAC therapy with newer imaging modalities may be of clinical significance in the early diagnosis, treatment, and prognosis of patients with sepsis-associated encephalopathy.

To elucidate the pathophysiological mechanism and therapeutic effects of NAC, we induced sepsis-associated encephalopathy in rats and studied the effects of NAC on neuroimaging results (Glu CEST and DKI). Additionally, we provide new neuroimaging information and diagnostic strategies and treatment for sepsis-associated encephalopathy.

RESULTS AND DISCUSSION

Sepsis-associated encephalopathy is one of the most common complications of sepsis and is associated with increased mortality and poor prognosis in patients with sepsis; thus, early diagnosis and treatment are of clinical relevance. The pathogenesis is multifactorial and involves neuroinflammation, destruction of the blood–brain barrier, and changes in the neurotransmitter levels.¹³ NAC is an anti-inflammatory and antioxidant substance that plays an essential role in neurological diseases. This study aimed to investigate the effects of NAC on sepsis-associated encephalopathy-related pathological features in a rat model and detect early pathological changes in

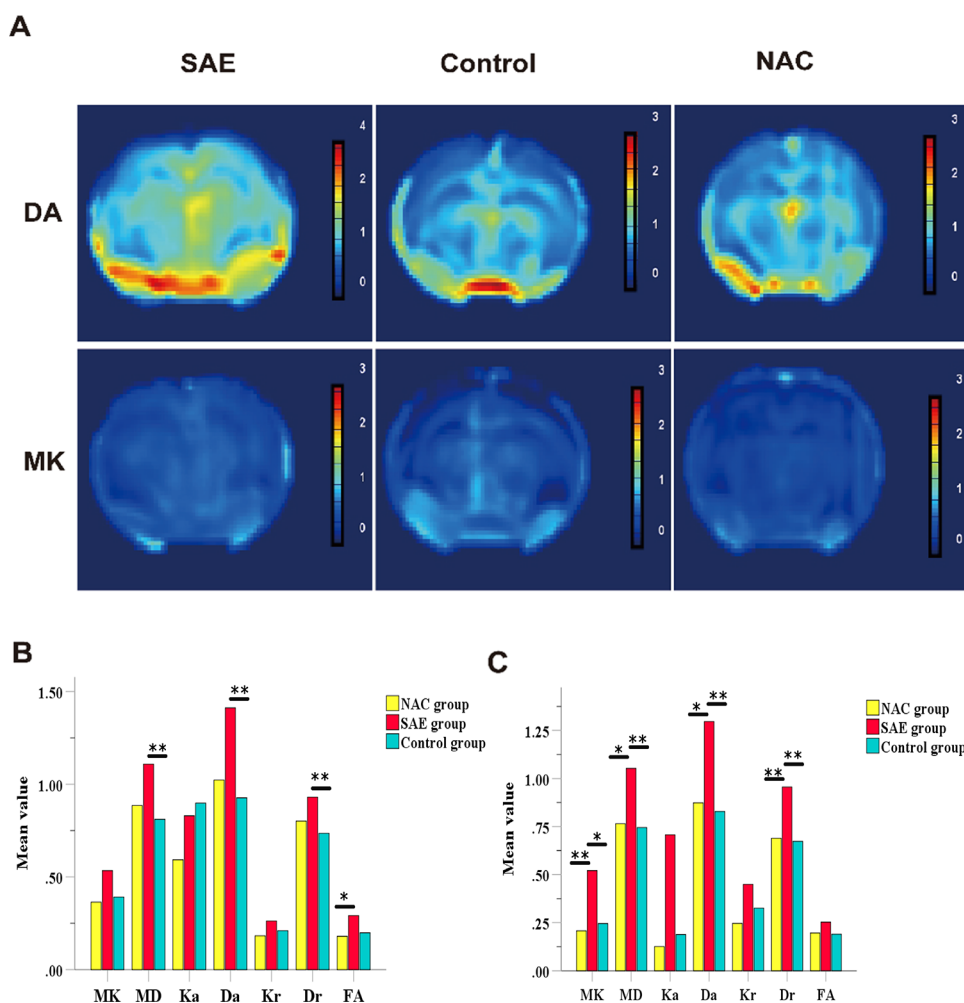


Figure 3. Results of DKI. (A) Da and MK color maps of the three study groups. (B) Statistical plots of different parameters of DKI in the cortical areas for the three study groups. (C) Statistical plots of the different parameters of DKI in the hippocampal areas for the three study groups. Da: Axial diffusion; MK: Mean kurtosis; DKI: Diffusion kurtosis imaging.

the brain using various MRI modalities. NAC treatment resulted in significant protective effects against sepsis-associated encephalopathy pathologies in the rats, while the brain-related changes were correlatively detected using DKI and Glu CEST.

NAC Improves Behavioral Performance in Sepsis-Associated Encephalopathy. Compared with the control group, the sepsis-associated encephalopathy group was more likely to be at the periphery of the black box, whereas the NAC group was more likely to be at the center of the box (Figure 1A). Furthermore, the standing scores of the sepsis-associated encephalopathy group were significantly lower than those of the control ($P = 0.001$, Kruskal–Wallis test) and NAC groups ($P = 0.033$, Kruskal–Wallis test). Compared with the control group, the NAC group also showed improvements in the total distance, average speed, crossing score, activity time, and standing time (Figure 1B).

Imaging Changes in the Brain after NAC Treatment in Rats. The Glu CEST values in the sepsis-associated encephalopathy group (15.20 ± 0.79) were significantly higher than those in the NAC (11.74 ± 0.37) ($P = 0.010$, Kruskal–Wallis test) and control (11.93 ± 1.63) ($P = 0.001$, Kruskal–Wallis test) groups (Figure 2A,B). Furthermore, the sepsis-associated encephalopathy group showed a higher percentage of Glu CEST contrast than the other two groups. The Glu

CEST distribution in the cortical area of the rats in the sepsis-associated encephalopathy group was apparent.

Imaging analysis revealed that the MK, Da, MD, and Dr values in the cortex were significantly higher in the sepsis-associated encephalopathy group than those in the NAC and control groups. Similarly, the Da, MD, Dr, and FA values in the hippocampus were significantly higher in the sepsis-associated encephalopathy group than those in the control group (Figure 3).

NAC Treatment Reduced the Inflammatory Response Related to Sepsis-Associated Encephalopathy.

The levels of TNF- α , an inflammatory response marker protein, were significantly ($P < 0.01$) higher in the sepsis-associated encephalopathy group than those in the control group. After NAC treatment, the TNF- α levels of the sepsis-associated encephalopathy group decreased and were similar to those of the control group (Figure 4A). These results indicate that NAC possibly reduces the expression of TNF- α and inhibits inflammation. To further evaluate the effects of NAC on improving the intracellular antioxidant capacity and reducing the levels of inflammatory injury, we also analyzed the serum glutathione concentrations before and after NAC treatment and found that the serum glutathione levels increased significantly from $18.49 \pm 6.93 \mu\text{M}$ before treatment to

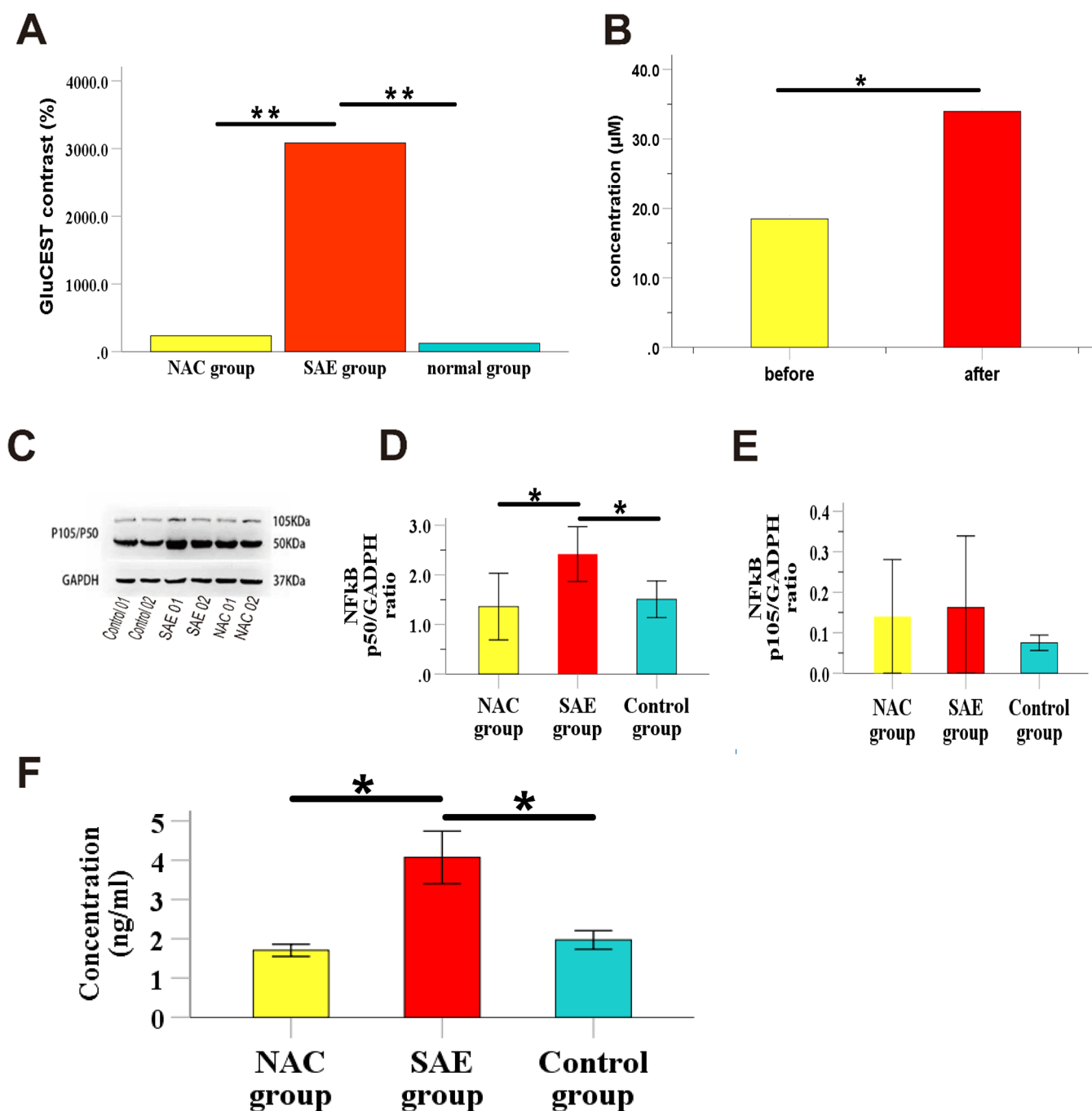


Figure 4. Analysis of the biochemical test results. (A) TNF- α levels for the three study groups. (B) Glutathione levels before and after treatment with NAC in sepsis-associated encephalopathy. (C) Expression levels of NF κ B (p50/105) protein for the three study groups. (D) Statistical results of NF κ B (p50) protein for the three study groups. (E) Statistical results of NF κ B (p105) protein for the three study groups. (F) EB staining results for the three study groups. TNF- α : Tumor necrosis factor α ; NF κ B = Nuclear factor kappa B; NAC: N-acetylcysteine; EB: Evans blue.

$33.95 \pm 11.49 \mu\text{M}$ after treatment ($P = 0.33$, t -test) (Figure 4B).

Similar to the results of the TNF- α levels, higher NF κ B (p50) expression levels were noted in the sepsis-associated encephalopathy group than in the control group, and the levels significantly decreased after NAC treatment (Figure 4C–E).

To explore the association between sepsis-associated encephalopathy-related immune mechanisms and brain imaging changes, we performed a correlation analysis of the TNF- α levels with the DKI parameters in the cortical and hippocampal regions. A correlation was observed among various DKI

parameters and the TNF- α levels in the hippocampus and cortex (Figure 5); Da ($r = 0.822$, $P = 0.00$, Spearman correlation analysis). MD ($r = 0.756$, $P = 0.00$, Spearman correlation analysis) were more closely related to the cortex and hippocampus regions, respectively.

NAC Improves the Permeability of the Blood–Brain Barrier. The sepsis-associated encephalopathy group ($4.07 \pm 0.64 \text{ ng/mL}$) showed a higher Evans blue (EB) concentration than the control group ($1.97 \pm 0.23 \text{ ng/mL}$) ($P = 0.001$, Tamhane's T2 test). After NAC treatment, the EB

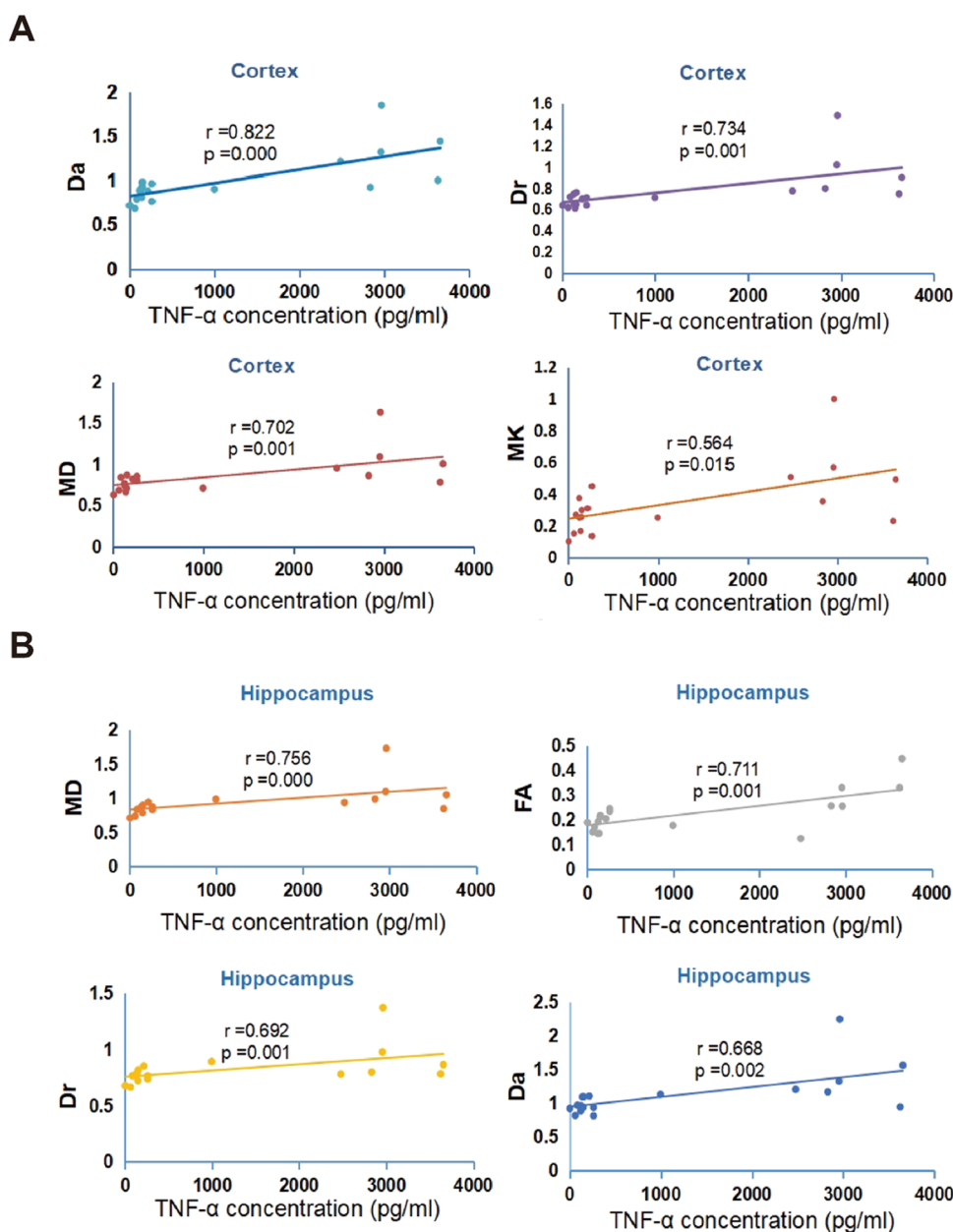


Figure 5. Graph of the statistical results of correlation analysis. Correlation analysis of TNF- α and DKI parameters in the cortex (A) and hippocampus (B). TNF- α : Tumor necrosis factor α ; DKI: Diffusion kurtosis imaging.

concentration decreased significantly (1.70 ± 0.15 ng/mL) ($P = 0.001$, Tamhane's T2 test) (Figure 4F).

Effects of NAC on the Nervous System in Sepsis-Associated Encephalopathy. Besides neurons, the nervous system also contains glial cells (such as the astrocytes and microglia). Astrocytes play an essential role in regulating the immune processes, Glu release, and neurovascular contractility. To further investigate the effects of NAC on the astrocytes, we detected the glial fibrillary acidic protein (GFAP) in different groups. Although the total number of astrocytes did not change significantly among the groups, the density and staining intensity in the sepsis-associated encephalopathy group were lower than those in the control group; however, the NAC group showed an intermediate staining profile (Figure 6A). We also performed Nissl staining to assess the changes in the neurons in the hippocampus region of the brain and found that the Nissl bodies were smaller and stained lighter in the sepsis-

associated encephalopathy group than those in the control group. Further, the NAC group had an intermediate staining profile (Figure 6B,C).

Patients with sepsis-associated encephalopathy are known to have anxiety and depression, which are related to cognitive impairment due to damage in the hippocampus region of the brain.¹⁴ In the OFT, we observed that rats injected with lipopolysaccharides (LPS) were more active at the periphery of the field and had more obvious anxiety and depression; NAC treatment alleviated these symptoms. In such cases, NAC may normalize the release of neurotransmitters from the Glu nerve endings, restoring metabolism to achieve the antioxidant and antidepressant effects.¹⁵ Previous studies have also suggested that NAC may act as an antidepressant by regulating the α -amino-3-hydroxy-5-methyl-4-isoxazole-propionic acid receptor, metabolic Glu receptor, and Glu exchanger of the astrocytes.^{16,17} Furthermore, the antidepressant effect of chronic

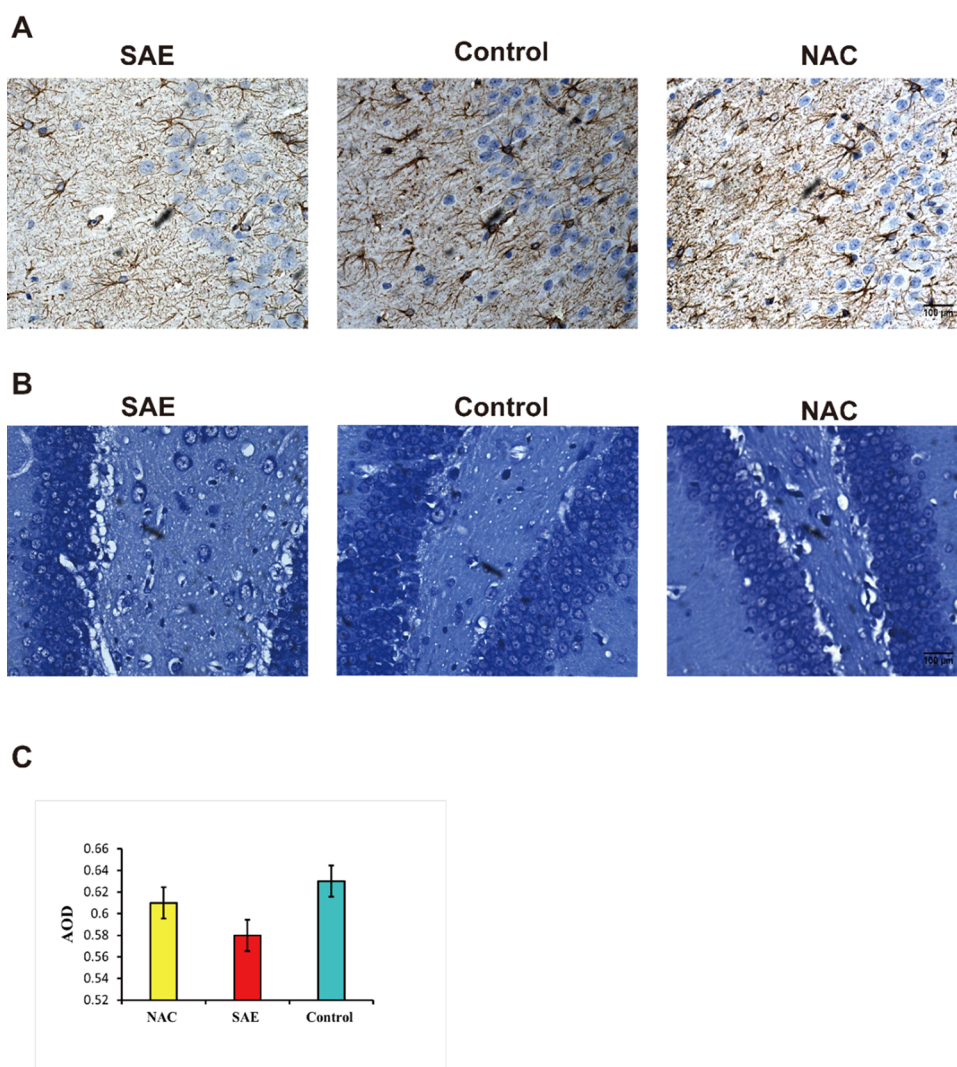


Figure 6. Pathological findings in different groups of rats. (A) Immunohistochemical staining of GFAP in different groups of rats. (B) Nissl staining of different groups of rats. (C) Mean optical density of different groups of rats with Nissl staining. GFAP: glial fibrillary acidic protein.

NAC treatment may be related to the loss of average volume in the hippocampal CA1, dentate gyrus, and hippocampal pyramidal subregion. NAC has also been shown to restore the decline of hippocampal monoamine levels and enhance metabolism in the hippocampus.^{18,19}

During sepsis-associated encephalopathy, Glu metabolism-related changes occurred early in the disease (within 24 hours); Glu-related excitatory toxicity occurs when Glu is over-released with insufficient synaptic clearance and may aggravate injury.²⁰ In the early stages of sepsis-associated encephalopathy, detecting early abnormalities using conventional imaging modalities, such as MRI, is challenging. The combined use of emerging modalities (DKI and Glu CEST) may help in the successful detection and monitoring of sepsis-associated encephalopathy-related features in the early stage. The results of this study demonstrated the utility of Glu CEST in detecting the pathologies before and after NAC treatment. In addition, our results also showed that glutathione levels were increased after NAC treatment. Glutathione possibly combines with free radicals and heavy metals to transform harmful toxins into harmless substances and excretes them out of the body.²¹ Glutathione is regulated by excitatory amino acid carrier 1 on the cell membrane, which encourages extracellular Glu and

cysteine to enter the cell for glutathione synthesis, thereby reducing the excitatory toxicity of Glu and improving the antioxidant level in cells.^{22,23} The primary physiological function of glutathione is to scavenge free radicals in the human body. As an essential antioxidant, glutathione protects the sulfhydryl groups in many proteins and enzymes.²⁴ NAC might be involved in the molecular synthesis and regulation of glutathione during inflammation, thereby improving the antioxidant levels in cells, alleviating cytotoxic damage, and reducing brain injury in sepsis-associated encephalopathy.^{25,26}

Glu is converted into glutamine in the astrocytes and recycled into neurons to synthesize Glu and maintain synaptic transmission. Hence, Glu levels may be closely related to the astrocyte function.²⁷ Glu levels are associated with dysfunction in the astrocytes, which release transmitters such as ATP and adenosine that regulate synaptic transmission and plasticity. Continuous synaptic transmission is regulated by the astrocytes' neurotransmitter uptake transporters that remove Glu from the synaptic cleft.²⁸ Astrocytes are also part of the blood–brain barrier and maintain the homeostasis of the CNS. It has been reported that LPS stimulation causes extensive structural changes in the astrocytes, such as structural remodeling and loss of foot processes, resulting in blood–

brain barrier destruction.²⁹ Higher glutathione levels in the astrocytes can improve the blood–brain barrier function by maintaining tight junction protein in the brain tissue and inhibiting injury-induced tight junction phosphorylation.³⁰ Our GFAP immunohistochemistry and Nissl staining results showed that NAC reduced sepsis-associated encephalopathy-related nervous tissue damage, which may be related to alleviating the structural damage of the astrocytes. The changes in blood–brain barrier permeability and the regulation of inflammatory factors by sepsis-associated encephalopathy may be related to the foot process swelling and astrocyte dysfunction, which may also affect the release of neurotransmitters (Glu). Our EB results indicate that the sepsis-associated encephalopathy group had the most serious impairment of the blood–brain barrier permeability, while NAC alleviated this damage. We speculate that the salvage effects of NAC on the astrocytes may be the possible mechanism behind this observation as astrocytes are important components of the blood–brain barrier.

The parameters of DTI are related to the demyelination changes in the brain under physiological or pathological conditions, while the parameters of DKI are more complex. DKI technology is an extension of DTI, and DKI is suitable for grasping functional tissue microstructural changes under non-normal distribution.^{31,32} Recent studies using electron microscopy have detected less myelination in the subcortical white matter and axons of the hippocampus region during sepsis, explaining the reduced myelin formation in sepsis-associated encephalopathy as detected by DTI.³³ Moreover, the myelin sheath in the prefrontal cortex and hippocampal axons is reduced during sepsis, possibly as the differentiation/maturation of the microglia is affected and the expression of transcription factors Olig1 and Olig2 is inhibited.³⁴ Our results suggest damage in the brain microstructures of animals in the sepsis-associated encephalopathy group, which may be related to the pathophysiological mechanism. Furthermore, these results also suggest that NAC treatment had a protective effect on the animals from the deleterious effects of sepsis-associated encephalopathy. The most critical parameter in DKI is MK, which is independent of the spatial orientation of the organizational structure. A larger MK value indicates a more complex structure with a more pronounced diffusion limit of abnormal distribution of water molecules. Therefore, we employed DKI to investigate early signals related to sepsis-associated encephalopathy and found that MK in the cortical region was significantly higher in the sepsis-associated encephalopathy group than those in the NAC and control groups. Previous studies have also confirmed that the pathophysiological mechanism of MK may be related to the proliferation of reactive astrocytes after brain injury.³⁵ In addition, previous studies have also shown that TNF- α blockers can inhibit demyelinating changes in the CNS. In this study, we also found a significant correlation between DKI and TNF- α levels that indicates that NAC may improve neuroinflammatory progression by inhibiting TNF- α levels and that DKI has excellent potential to detect sepsis-associated encephalopathy-related early inflammatory markers.

Life-threatening organ dysfunction caused by abnormal immune response is often a fundamental cause of the onset and development of sepsis. NAC can inhibit sepsis-associated encephalopathy-related inflammation and enhance the antioxidant levels. In the beginning of sepsis-associated encephalopathy, associated inflammatory signals can reach different

brain areas by stimulating peripheral nerves and blood circulation. Astrocytes play a crucial role in driving inflammatory brain injury by monitoring and integrating inflammatory signals and coordinating the role of immune cells in the CNS.^{36–39} Activation of astrocytes in the brain tissues can be detected in the early stage of sepsis. The activated astrocytes can release various inflammatory mediators (e.g., TNF- α , IL-1 β , IL-6, IL-18) and enhance the expression of NF κ B, promoting the inflammatory process.⁴⁰ Excessive production of inflammatory cytokines, such as TNF- α , leads to further worsening of neuroinflammation and massive loss of brain cells. TNF- α appears to be a key mediator of sepsis-associated encephalopathy, directly associated with blood–brain barrier disruption, brain edema, neutrophil infiltration, astrocyte proliferation, and brain cell apoptosis. TNF- α is a mononuclear factor mainly produced by the monocytes and macrophages.⁴¹ The level of TNF- α is positively correlated with the severity of inflammation, and its gene expression is regulated by NF κ B.⁴² NF κ B is a protein complex that controls transcribed DNA, cytokine production, and cell survival. It plays a crucial role in regulating the immune response to infection and is identified as a vital mediator of the blood–brain barrier in sepsis-associated encephalopathy. The NF- κ B family consists of five members: RelA (p65), RelB, c-Rel, NF- κ B1 (p50/p105), and NF- κ B2 (p52/p100). These members form isomers or heterodimers that play different roles in regulating the expression of inflammatory genes, cell survival, and neuron differentiation in the CNS.⁴³ Bacterial LPS activates NF- κ B by binding to the toll-like receptor 4 on the surface of the cell membrane and degrading the NF- κ B inhibitor family.⁴⁴ The classical pathway starts with the activation of NF κ B1(p50/p105), which then enters the nucleus, binds to the DNA, and promotes the transcription of NF κ B dependent genes, such as NLRP3, Pro-IL-1 β , and Pro-IL-18, subsequently triggering the inflammasome and causing cellular damage, such as mitochondrial damage and oxidative stress.^{45,46} However, this phenomenon was not observed in mice lacking TNF-receptor 1 gene.⁴⁷

This study is limited by the fact that clinical conditions are often complex, and many patients have other underlying diseases. Therefore, it is difficult for ordinary animal models to simulate the symptoms seen in different patients accurately. However, it can provide a basic background for further clinical studies.

In conclusion, this study showed that emerging magnetic resonance molecular imaging technology modalities, such as DKI and Glu CEST, may be used to diagnose and detect pathological features in the early stages of sepsis-associated encephalopathy. Noninvasive *in vivo* detection of microstructural molecular metabolic changes in the brain of patients with sepsis-associated encephalopathy in combination with imaging holds great promise for clinical application, which might improve early clinical diagnosis and patient cure rates. Furthermore, we also demonstrated that NAC improved the behavioral responses in rats, reduced inflammatory reactions, enhanced blood–brain barrier permeability, and rescued animals from the deleterious effects associated with sepsis-associated encephalopathy, which also provides new clinical strategies in the treatment and prognostic assessment of sepsis-associated encephalopathy.

METHODS

Sepsis-Associated Encephalopathy Rat Model and Groups.

All animal experiments were performed in accordance with the ARRIVE guidelines and the National Institutes of Health guide for the care and use of Laboratory animals (NIH Publications No. 8023, revised 1978) and approved by the Animal Ethics Committee of Shantou University Medical College (2020-15), China. Sixty healthy Sprague–Dawley rats (weighing 180–250 g, male and female) were randomly divided into three groups (each group $n \geq$ six animals): (1) Sepsis-associated encephalopathy group, where the rats were intraperitoneally injected with 10 mg/kg of LPS from *Escherichia coli* (O55:B5) (No. L2880, Sigma-Aldrich). The neurobiological scores (including auricular reflex, corneal reflex, rollover reflex, tail-flick reflex, and escape reflex) of the rats were assessed within 24 h, with 0 representing no reflex, 1 representing a reduced reflex (lack of reflex within 10 s), and 2 representing a normal reflex. A total score of ≥ 6 represented the sepsis-associated encephalopathy model rats;⁴⁸ (2) NAC group, where NAC (200 mg/kg) was injected through the tail vein for 1 week after the sepsis-associated encephalopathy model was established; and (3) control group, where the animals were intraperitoneally injected with saline (volume equal to that of the LPS injected in the sepsis-associated encephalopathy group).

Open-Field Test. OFT is a widely used method to evaluate the autonomous and exploratory behaviors and analyze the tension of animals in novel experimental environments.⁴⁹ The OFT device is a black box (100 cm \times 100 cm \times 40 cm) divided into a peripheral and a central square area. During the experiment, the animals received crossing and rearing scores for crossing different squares and standing on their hind legs, respectively. Furthermore, the total distance, average speed, activity time, standing time, and time of activity in the surrounding and central areas were computed automatically based on the animal track recorded by the camera. At the end of each experiment, the OFT device was cleaned using ethanol (75%) and dried to avoid residuals, such as animal urine, feces, and smell, which could affect the behavior of animals during the next test.

MRI Examinations. The animals were anesthetized with 1.5–2% isoflurane mixed with oxygen at a flow rate of 0.5–1 L/min and placed into the animal scaffold inside the volume coil of a 7.0-T MRI scanner. The brain was fixed with a special surface coil designed for rats. Respiration and heart rates were monitored using an MRI-compatible small animal monitoring system (SAII Technologies, Memphis, TN), and the structural and functional images of the rat brain were obtained using Glu CEST. The location maps of the three imaging planes were obtained during scanning. The target plane was located, and the region of interest was selected to scan the T2-weighted image as the structural phase. Single-shot echo planar imaging sequence with continuous-wave saturation pulse ($B_1 = 3.6 \mu\text{T}$, pulse width = 4 s) was used to obtain Glu CEST images with the following parameters for the selected plane: field of view = $37 \times 37 \text{ mm}^2$, slice thickness = 2 mm, $k_{\text{zero}} = 32$, shot = 1, repeat time (TR) = 6000 ms, echo time (TE) = 27.97 ms, matrix size = 64×64 . CEST images (a total of 121 images) were collected with $B_{\text{rms}} = 3.6 \mu\text{T}$ for frequencies ranging from -6.0 to $+6.0$ ppm from bulk water in a step size of 0.1 ppm. B_1 and water saturation shift referencing B_0 field maps were also acquired and used to correct the CEST maps as described previously.⁵⁰

The animals were also scanned using DKI with the following parameters: TR = 2000 ms, TE = 90.13 ms, $k_{\text{zero}} = 64$, repetitions = 1, shots = 1, matrix = 128×128 , slices = 1, thickness = 2 mm, gap = 0 mm, the diffusion sensitive gradient field applied direction was 15, the B values in each direction had three values (0, 1000, 2000 s/mm^2), and the scanning time was 36 min. Matlab 2016 (MathWorks, Natick, MA) and ImageJ (National Institutes of Health, Bethesda, MD) were used to post-process the CEST and DKI images.

Enzyme-Linked Immunosorbent Assay (ELISA). Venous blood was collected gently and quickly from the inner canthus of the orbit of the rats via a capillary tube to avoid eyeball injury. After standing and centrifugation, the blood samples were prepared for ELISA. The absorbance of total glutathione and TNF- α in the blood samples was

measured using an Enspire multifunctional microplate analyzer (PerkinElmer, Waltham, MA).

Western Blot. The rats in all three groups were anesthetized by intraperitoneally injecting 10% chloral hydrate (4 mL/kg). The thoracic cavity was incised to expose the location of the heart, and the left ventricle was placed with a suitable needle. Subsequently, the right auricle was cut open and perfused from the left ventricle with sterile saline (cooled to 4 °C). Finally, the head was severed, the brain was removed, and the brain tissue was separated on ice. The prepared animal samples were analyzed to detect proteins using western blotting, and the protein levels were quantified using ImageJ software.

Immunohistochemical Staining. Brain tissues from different groups of rats were prepared into paraffin sections for preservation. Paraffin sections were dewaxed in water and soaked in xylene and gradient alcohol (anhydrous, 95, 85, and 75% for 5 min, respectively). After microwaving, 3% hydrogen peroxide was added to block endogenous peroxidases, followed by rinsing and incubation with bovine serum albumin (5%) for 30 min and GFAP rabbit monoclonal antibodies (1:100) for 1 h at least. After washing with phosphate-buffered saline, the goat anti-rabbit antibody (1:1000) was added to each section and incubated for 30 min. Fresh 3,3'-diaminobenzidine (approximately 50 μL for each slide) was added after washing, and the slide was placed under the microscope for observation.

Evans Blue Staining. EB staining was used to evaluate the changes in the blood–brain barrier permeability using the method described previously. A 2% solution of EB was injected (2 mL/kg) into the tail vein (or femoral vein) of the animals, and the animals were weighed 30 min before euthanization. After anesthetizing animals with 10% chloral hydrate (0.3 mL/100 g), the thorax was opened, and approximately 200 mL of heparinized normal saline was injected into the heart. When the outflow fluid from the right atrium became clear, the perfusion was stopped, the head was decapitated, and the brains were weighed. After centrifugation, the supernatant was taken and the absorbances at 620 nm were measured using a spectrophotometer (Olympus, Japan).

Nissl Staining. Nissl staining was used to further evaluate the damage to the nervous system. Paraffin sections were successively dewaxed using xylene, anhydrous ethanol, 95% alcohol, 80% alcohol, 70% alcohol, and distilled water. The sections were subsequently washed with distilled water, dyed with 1% toluidine blue, washed with distilled water, differentiated with ethanol differentiation solution, and dehydrated with anhydrous ethanol and xylene before being sealed and observed under a microscope.

Statistical Analysis. All values are presented as mean \pm standard error of the mean. A value of $P < 0.05$ represented statistical significance. Two-sided statistical analysis was performed using SPSS 26.0 statistical software (SPSS, Inc., Chicago, IL). The Kolmogorov–Smirnov test was performed on all quantitative data to determine normal distribution. The Kruskal–Wallis test was used for the analysis of nonparametric data with multiple samples. The correlation between the samples was analyzed using Spearman correlation analysis.

ASSOCIATED CONTENT

Data Availability Statement

The authors state that anonymized data on which the article is based will be shared by request from any qualified investigator.

AUTHOR INFORMATION

Corresponding Author

Renhua Wu – Department of Radiology, The Second Affiliated Hospital, Shantou University Medical College, Shantou 515041 Guangdong, China; Phone: +86 13322772961; Email: rhwu@stu.edu.cn; Fax: +86 754 88915674

Authors

Yazhi Zhong – Department of Radiology, The Second Affiliated Hospital, Shantou University Medical College, Shantou 515041 Guangdong, China; Department of

Radiology, Huizhou Central People's Hospital, Huizhou 516001 Guangdong, China; orcid.org/0000-0002-3617-3566

Jitian Guan – Department of Radiology, The Second Affiliated Hospital, Shantou University Medical College, Shantou 515041 Guangdong, China; orcid.org/0000-0002-8910-7052

Yunfeng Ma – Department of Emergency, The Second Affiliated Hospital, Shantou University Medical College, Shantou 515041 Guangdong, China

Meiling Xu – Department of Emergency, The Second Affiliated Hospital, Shantou University Medical College, Shantou 515041 Guangdong, China

Yan Cheng – Department of Radiology, The Second Affiliated Hospital, Shantou University Medical College, Shantou 515041 Guangdong, China; Department of Radiology, The Second Hospital of Shandong University, Jinan 250033 Shandong, China

Liang Xu – Department of Radiology, The Second Affiliated Hospital, Shantou University Medical College, Shantou 515041 Guangdong, China; Department of Radiology, The Seventh Affiliated Hospital, Sun Yat-sen University, Shenzhen 518100 Guangdong, China; orcid.org/0000-0002-6381-7267

Yan Lin – Department of Radiology, The Second Affiliated Hospital, Shantou University Medical College, Shantou 515041 Guangdong, China

Xiaolei Zhang – Department of Radiology, The Second Affiliated Hospital, Shantou University Medical College, Shantou 515041 Guangdong, China

Complete contact information is available at:

<https://pubs.acs.org/10.1021/acscchemneuro.3c00180>

Author Contributions

*Y.Z. and J.G. contributed equally to this work. Y.Z.: writing—original draft preparation, methodology, visualization, conceptualization, data curation; J.G.: supervision, methodology; Y.M.: investigation; M.X.: investigation; Y.C.: writing—review & editing; L.X.: resources; Y.L.: formal analysis; X.Z.: software; R.W.: funding acquisition, project administration.

Funding

This work was supported by grants from the National Science Foundation of China (grant nos. 31870981 and 82020108016), 2020 LKSF Cross-Disciplinary Research (grant no. 2020LKSFMBME06), 2020 Li Ka Shing Foundation Cross-Disciplinary Research (grant no. 2020LKSF05D), Grant for Key Disciplinary Project of Clinical Medicine under the Guangdong High-Level University Development Program (grant no. 002-18120302), and Shenzhen Science and Technology Program (No. JCYJ20210324105806016).

Notes

The authors declare no competing financial interest.

ACKNOWLEDGMENTS

The authors acknowledge the Central Laboratory of Shantou University Medical College and Translational Medicine Center and The Second Affiliated Hospital of Shantou University Medical College, China.

ABBREVIATIONS

CEST, chemical exchange saturation transfer; Da, axial diffusion; DKI, diffusion kurtosis imaging; DTI, diffusion

tensor imaging; Dr, radial diffusion; EB, Evans blue; FA, fractional anisotropy; GFAP, glial fibrillary acidic protein; Glu, glutamate; IL-6, interleukin-6; Ka, axial kurtosis; Kr, radial kurtosis; LPS, lipopolysaccharides; MD, mean diffusivity; MK, mean kurtosis; NAC, *n*-acetylcysteine; NF κ B, nuclear factor kappa B; OFT, open-field test; TE, echo time; TNF- α , tumor necrosis factor α ; TR, repeat time

REFERENCES

- (1) Gofton, T. E.; Young, G. B. Sepsis-associated Encephalopathy. *Nat. Rev. Neurol.* **2012**, *8*, 557–566.
- (2) Shulyatnikova, T.; Verkhatsky, A. Astroglia in Sepsis Associated Encephalopathy. *Neurochem. Res.* **2020**, *45*, 83–99.
- (3) Peng, X.; Luo, Z.; He, S.; Zhang, L.; Li, Y. Blood-Brain Barrier Disruption by Lipopolysaccharide and Sepsis-Associated Encephalopathy. *Front Cell Infect. Microbiol.* **2021**, *11*, No. 768108.
- (4) Mazerand, A.; Righy, C.; Bouchereau, E.; Benghanem, S.; Bozza, F. A.; Sharshar, T. Septic-Associated Encephalopathy, a Comprehensive Review. *Neurotherapeutics* **2020**, *17*, 392–403.
- (5) Andica, C.; Kamagata, K.; Hatano, T.; Saito, Y.; Ogaki, K.; Hattori, N.; Aoki, S. MR Biomarkers of Degenerative Brain Disorders Derived from Diffusion Imaging. *J. Magn. Reson. Imaging* **2020**, *52*, 1620–1636.
- (6) Marrale, M.; Collura, G.; Brai, M.; Toschi, N.; Midiri, F.; La Tona, G.; Lo Casto, A.; Gagliardo, C. Physics, Techniques and Review of Neuroradiological Applications of Diffusion Kurtosis Imaging (DKI). *Clin. Neuroradiol.* **2016**, *26*, 391–403.
- (7) Dou, W.; Lin, C. E.; Ding, H.; Shen, Y.; Dou, C.; Qian, L.; Wen, B.; Wu, B. Chemical Exchange Saturation Transfer Magnetic Resonance Imaging and its Main and Potential Applications in Pre-Clinical and Clinical Studies. *Quant. Imaging Med. Surg.* **2019**, *9*, 1747–1766.
- (8) Li, R.; Dai, Z.; Hu, D.; Zeng, H.; Fang, Z.; Zhuang, Z.; Xu, H.; Huang, Q.; Cui, Y.; Zhang, H. Mapping the Alterations of Glutamate Using Glu-Weighted CEST MRI in a Rat Model of Fatigue. *Front. Neurol.* **2020**, *11*, No. 589128.
- (9) Bagga, P.; Pickup, S.; Crescenzi, R.; Martinez, D.; Borthakur, A.; D'Aquila, K.; Singh, A.; Verma, G.; Detre, J. A.; Greenberg, J.; Hariharan, H.; Reddy, R. In Vivo GluCEST MRI, Reproducibility, Background Contribution and Source of Glutamate Changes in the MPTP Model of Parkinson's Disease. *Sci. Rep.* **2018**, *8*, No. 2883.
- (10) Tardiolo, G.; Bramanti, P.; Mazzon, E. Overview on the Effects of N-Acetylcysteine in Neurodegenerative Diseases. *Molecules* **2018**, *23*, 3305.
- (11) Ortolani, O.; Conti, A.; De Gaudio, A. R.; Moraldi, E.; Novelli, G. P. [Glutathione and N-Acetylcysteine in the Prevention of Free-Radical Damage in the Initial Phase of Septic Shock]. *Recenti Prog. Med.* **2002**, *93*, 125–129.
- (12) Chertoff, J. N-Acetylcysteine's Role in Sepsis and Potential Benefit in Patients With Microcirculatory Derangements. *J. Intensive Care Med.* **2018**, *33*, 87–96.
- (13) Maramattom, B. V. Sepsis Associated Encephalopathy. *Neurol. Res.* **2007**, *29*, 643–646.
- (14) Semmler, A.; Okulla, T.; Sastre, M.; Dumitrescu-Ozimek, L.; Heneka, M. T. Systemic Inflammation Induces Apoptosis with Variable Vulnerability of Different Brain Regions. *J. Chem. Neuroanat.* **2005**, *30*, 144–157.
- (15) Deutschenbaur, L.; Beck, J.; Kiyhankhadiv, A.; Mühlhauser, M.; Borgwardt, S.; Walter, M.; Hasler, G.; Sollberger, D.; Lang, U. E. Role of Calcium, Glutamate and NMDA in Major Depression and Therapeutic Application. *Prog. Neuropsychopharmacol. Biol. Psychiatry* **2016**, *64*, 325–333.
- (16) Costa-Campos, L.; Herrmann, A. P.; Pilz, L. K.; Michels, M.; Noetzel, G.; Elisabetsky, E. Interactive Effects of N-Acetylcysteine and Antidepressants. *Prog. Neuropsychopharmacol. Biol. Psychiatry* **2013**, *44*, 125–130.
- (17) Linck, V. M.; Costa-Campos, L.; Pilz, L. K.; Garcia, C. R.; Elisabetsky, E. AMPA Glutamate Receptors Mediate the Anti-

depressant-like Effects of N-Acetylcysteine in the Mouse Tail Suspension Test. *Behav. Pharmacol.* **2012**, *23*, 171–177.

(18) Chakraborty, S.; Tripathi, S. J.; Srikumar, B. N.; Raju, T. R.; Shankaranarayana Rao, B. S. N-Acetyl Cysteine Ameliorates Depression-Induced Cognitive Deficits by Restoring the Volumes of Hippocampal Subfields and Associated Neurochemical Changes. *Neurochem. Int.* **2020**, *132*, No. 104605.

(19) Chakraborty, S.; Tripathi, S. J.; Raju, T. R.; Shankaranarayana Rao, B. S. Mechanisms Underlying Remediation of Depression-Associated Anxiety by Chronic N-Acetyl Cysteine Treatment. *Psychopharmacology* **2020**, *237*, 2967–2981.

(20) Blanco-Suárez, E.; Caldwell, A. L.; Allen, N. J. Role of Astrocyte-Synapse Interactions in CNS Disorders. *J. Physiol.* **2017**, *595*, 1903–1916.

(21) Bachhawat, A. K.; Thakur, A.; Kaur, J.; Zulkifli, M. Glutathione Transporters. *Biochim. Biophys. Acta* **2013**, *1830*, 3154–3164.

(22) Aoyama, K.; Nakaki, T. Glutathione in Cellular Redox Homeostasis, Association with the Excitatory Amino Acid Carrier 1 (EAAC1). *Molecules* **2015**, *20*, 8742–8758.

(23) Aoyama, K. Glutathione in the Brain. *Int. J. Mol. Sci.* **2021**, *22*, 5010.

(24) Homma, T.; Fujii, J. Application of Glutathione as Anti-Oxidative and Anti-Aging Drugs. *Curr. Drug Metab.* **2015**, *16*, 560–571.

(25) Maheswari, E.; Saraswathy, G. R.; Santhranii, T. Hepatoprotective and Antioxidant Activity of N-Acetyl Cysteine in Carbamazepine-Administered Rats. *Indian J. Pharmacol.* **2014**, *46*, 211–215.

(26) Nouri, A.; Heidarian, E.; Nikoukar, M. Effects of N-Acetyl Cysteine on Oxidative Stress and TNF- α Gene Expression in Diclofenac-Induced Hepatotoxicity in Rats. *Toxicol. Mech. Methods* **2017**, *27*, 561–567.

(27) Fullana, N.; Gasull-Camós, J.; Tarrés-Gatius, M.; Castañé, A.; Bortolozzi, A.; Artigas, F. Astrocyte Control of Glutamatergic Activity, Downstream Effects on Serotonergic Function and Emotional Behavior. *Neuropharmacology* **2020**, *166*, No. 107914.

(28) Duan, S.; Anderson, C. M.; Stein, B. A.; Swanson, R. A. Glutamate Induces Rapid Upregulation of Astrocyte Glutamate Transport and Cell-Surface Expression of GLAST. *J. Neurosci.* **1999**, *19*, 10193–10200.

(29) Cardoso, F. L.; Herz, J.; Fernandes, A.; Rocha, J.; Sepodes, B.; Brito, M. A.; McGavern, D. B.; Brites, D. Systemic Inflammation in Early Neonatal Mice Induces Transient and Lasting Neurodegenerative Effects. *J. Neuroinflammation* **2015**, *12*, 82.

(30) Huang, S. F.; Othman, A.; Koshkin, A.; Fischer, S.; Fischer, D.; Zamboni, N.; Ono, K.; Sawa, T.; Ogunshola, O. O. Astrocyte Glutathione Maintains Endothelial Barrier Stability. *Redox. Biol.* **2020**, *34*, No. 101576.

(31) Jensen, J. H.; Helpert, J. A.; Ramani, A.; Lu, H.; Kaczynski, K. Diffusional Kurtosis Imaging, the Quantification of Non-Gaussian Water Diffusion by Means of Magnetic Resonance Imaging. *Magn. Reson. Med.* **2005**, *53*, 1432–1440.

(32) Wu, E. X.; Cheung, M. M. MR Diffusion Kurtosis Imaging for Neural Tissue Characterization. *NMR Biomed.* **2010**, *23*, 836–848.

(33) Huang, P.; Chen, X.; Hu, X.; Zhou, Q.; Lin, L.; Jiang, S.; Fu, H.; Xiong, Y.; Zeng, H.; Fang, M.; Chen, C.; Deng, Y. Experimentally Induced Sepsis Causes Extensive Hypomyelination in the Prefrontal Cortex and Hippocampus in Neonatal Rats. *Neuromolecular Med.* **2020**, *22*, 420–436.

(34) Kemanetzoglou, E.; Andreadou, E. CNS Demyelination with TNF- α Blockers. *Curr. Neurol. Neurosci. Rep.* **2017**, *17*, 36.

(35) Zhuo, J.; Xu, S.; Proctor, J. L.; Mullins, R. J.; Simon, J. Z.; Fiskum, G.; Gullapalli, R. P. Diffusion Kurtosis as an In Vivo Imaging Marker for Reactive Astroglia in Traumatic Brain Injury. *NeuroImage* **2012**, *59*, 467–477.

(36) Sofroniew, M. V. Multiple Roles for Astrocytes as Effectors of Cytokines and Inflammatory Mediators. *Neuroscientist* **2014**, *20*, 160–172.

(37) Giaume, C.; Kirchhoff, F.; Matute, C.; Reichenbach, A.; Verkhratsky, A. Glia: the Fulcrum of Brain Diseases. *Cell Death Differ.* **2007**, *14*, 1324–1335.

(38) Verkhratsky, A.; Parpura, V. Astroglipathology in Neurological, Neurodevelopmental and Psychiatric Disorders. *Neurobiol. Dis.* **2016**, *85*, 254–261.

(39) Verkhratsky, A.; Zorec, R.; Parpura, V. Stratification of Astrocytes in Healthy and Diseased Brain. *Brain Pathol.* **2017**, *27*, 629–644.

(40) Bellaver, B.; Dos Santos, J. P.; Leffa, D. T.; Bobermin, L. D.; Roppa, P. H. A.; da Silva Torres, I. L.; Gonçalves, C. A.; Souza, D. O.; Quincozes-Santos, A. Systemic Inflammation as a Driver of Brain Injury, the Astrocyte as an Emerging Player. *Mol. Neurobiol.* **2018**, *55*, 2685–2695.

(41) Zelová, H.; Hošek, J. TNF- α Signalling and Inflammation, Interactions Between Old Acquaintances. *Inflamm. Res.* **2013**, *62*, 641–651.

(42) Oeckinghaus, A.; Ghosh, S. The NF- κ B Family of Transcription Factors and its REGULATION. *Cold Spring Harb. Perspect. Biol.* **2009**, *1*, No. a000034.

(43) Liu, T.; Zhang, L.; Joo, D.; Sun, S. C. NF- κ B Signaling in Inflammation. *Signal Transduct. Target Ther.* **2017**, *2*, No. 17023.

(44) Gao, Q.; Hernandez, M. S. Sepsis-Associated Encephalopathy and Blood-Brain Barrier Dysfunction. *Inflammation* **2021**, *44*, 2143–2150.

(45) Hoesel, B.; Schmid, J. A. The Complexity of NF- κ B Signaling in Inflammation and Cancer. *Mol. Cancer* **2013**, *12*, 86.

(46) Diaz-Vivancos, P.; de Simone, A.; Kiddle, G.; Foyer, C. H. Glutathione-Linking Cell Proliferation to Oxidative Stress. *Free Radic. Biol. Med.* **2015**, *89*, 1154–1164.

(47) Alexander, J. J.; Jacob, A.; Cunningham, P.; Hensley, L.; Quigg, R. J. TNF is a Key Mediator of Septic Encephalopathy Acting Through its Receptor, TNF Receptor-1. *Neurochem. Int.* **2008**, *52*, 447–456.

(48) Luo, R. Y.; Luo, C.; Zhong, F.; Shen, W. Y.; Li, H.; Hu, Z. L.; Dai, R. P. ProBDNF Promotes Sepsis-Associated Encephalopathy in mice by Dampening the Immune Activity of Meningeal CD4(+) T Cells. *J. Neuroinflammation* **2020**, *17*, No. 169.

(49) Kuniishi, H.; Ichisaka, S.; Yamamoto, M.; Ikubo, N.; Matsuda, S.; Futora, E.; Harada, R.; Ishihara, K.; Hata, Y. Early Deprivation Increases High-Leaning Behavior, a Novel Anxiety-Like Behavior, in the Open Field Test in Rats. *Neurosci. Res.* **2017**, *123*, 27–35.

(50) Poblador Rodriguez, E.; Moser, P.; Dymerska, B.; Robinson, S.; Schmitt, B.; van der Kouwe, A.; Gruber, S.; Trattnig, S.; Bogner, W. A Comparison of Static and Dynamic $\Delta B(0)$ Mapping Methods for Correction of CEST MRI in the Presence of Temporal B(0) Field Variations. *Magn. Reson. Med.* **2019**, *82*, 633–646.